Plant Biotechnology Journal
Open Access

Plant Biotechnology Journal (2023) **21**, pp. 931–942 doi: 10.1111/pbi.14004

The MYB transcription factor *Seed Shattering 11* controls seed shattering by repressing lignin synthesis in African rice

Jing Ning[1], Wei He[1], Linhua Wu[1], Leqin Chang[1], Min Hu[1], Yongcai Fu[1], Fengxia Liu[2], Hongying Sun[1], Ping Gu[1], Marie-Noelle Ndjiondjop[3], Chuanqing Sun[2] and Zuofeng Zhu[1,*]

[1]*National Center for Evaluation of Agricultural Wild Plants (Rice), Department of Plant Genetics and Breeding, China Agricultural University, Beijing, China*
[2]*State Key Laboratory of Plant Physiology and Biochemistry, China Agricultural University, Beijing, China*
[3]*Africa Rice Center, Cotonou, Benin*

Received 2 February 2022;
revised 20 December 2022;
accepted 30 December 2022.
**Correspondence* (Tel +86 10 62732558; fax + 86 10 62731811; email zhuzf@cau.edu.cn (Z.Z))

Keywords: African rice, seed shattering, map-based cloning, gene editing.

Summary

African cultivated rice (*Oryza glaberrima* Steud.) was domesticated from its wild progenitor species (*Oryza barthii*) about 3000 years ago. Seed shattering is one of the main constraints on grain production in African cultivated rice, which causes severe grain losses during harvest. By contrast, Asian cultivated rice (*Oryza sativa*) displays greater resistance to seed shattering, allowing higher grain production. A better understanding in regulation of seed shattering would help to improve harvesting efficiency in African cultivated rice. Here, we report the map-based cloning and characterization of *OgSH11*, a MYB transcription factor controlling seed shattering in *O. glaberrima*. *OgSH11* represses the expression of lignin biosynthesis genes and lignin deposition by binding to the promoter of *GH2*. We successfully developed a new *O. glaberrima* material showing significantly reduced seed shattering by knockout of *SH11* in *O. glaberrima* using CRISPR-Cas9 mediated approach. Identification of *SH11* not only supplies a new target for seed shattering improvement in African cultivated rice, but also provides new insights into the molecular mechanism of abscission layer development.

Introduction

There are 1.1 billion people living in Sub-Saharan Africa and over 0.7 billion of them are suffering from moderate or severe food insecurity (data from FAO, 2021). By 2050, the population is expected to exceed 1.5 billion in this region (van Ittersum *et al.*, 2016). Therefore, improving agricultural productivity is critical to reducing the risk of hunger derived from a rapidly growing population in this region.

Rice is one of the most important crops in the world, which provides staple food for more than half of the world's population. There are two cultivated rice species, Asian cultivated rice (*Oryza sativa* L.) and African cultivated rice (*Oryza glaberrima* Steud.), which were independently domesticated from the wild progenitor species *Oryza rufipogon* and *Oryza barthii*, respectively (Meyer *et al.*, 2016). Due to the lack of modern breeding scheme, African cultivated rice has low grain production; hence, it is being replaced by higher yield Asian cultivated rice (*O. sativa*). However, in marginal areas under poor crop management, *O. glaberrima* is still favoured by farmers for its tolerance to multiple biotic and abiotic stress such as high temperature, Rice Yellow Mottle Virus (RYMV), drought, flood and weeds (Jones *et al.*, 1997; Li *et al.*, 2015; Linares, 2002; Thiemele *et al.*, 2010; Zhang *et al.*, 2022).

Strong seed shattering is one of the major causes of low productivity in *O. glaberrima*, which leads to severe grain loss during harvest (Montcho *et al.*, 2013). On the contrary, resistance to seed shattering in *O. sativa* allows high grain production. Therefore, a better understanding on how this trait is differently regulated between African cultivated rice (*O. glaberrima*) and Asian cultivated rice (*O. sativa*) will provide a basis for improving grain production in African cultivated rice.

Loss of seed shattering is one of the key steps during crop domestication. Several genes and mutations responsible for this trait have been identified in rice. *SH4* encodes a MYB transcription factor, and selection of the C to T mutant of *sh4* led to a significant decrease in seed shattering during the domestication of *O. sativa* (Li *et al.*, 2006). Another major QTL, *qSH1*, encodes a BEL1-type homeobox transcription factor and selection for an SNP lying in the 12-kb upstream of *qSH1* resulted in a further decrease of seed shattering in *O. sativa* subsp. *japonica* (Konishi *et al.*, 2006).

Two major genes, *GL4* and *SH3*, were selected during the domestication of *O. glaberrima*. *GL4* is the homologous gene of *SH4*, and a C to T mutant of *gl4* led to the early appearance of a termination codon, resulting in the loss of seed shattering and smaller grain size (Wu *et al.*, 2017). *SH3* encodes a YABBY family transcription factor, and selection for a 45-kb deletion around *SH3* led to loss of seed shattering during *O. glaberrima* domestication (Lv *et al.*, 2018). These findings provide important insights into the molecular mechanisms underlying seed shattering domestication in rice.

In addition, previous studies have identified several genetic factors controlling seed shattering in rice, such as *SHAT1*, *SH5*, *OsCPL1*, *SSH1* and *OsGRF4*, which perform important roles in the development of the abscission layer (Ji *et al.*, 2010; Jiang

et al., 2019; Sun *et al*., 2016; Yoon *et al*., 2014; Zhou *et al*., 2012). However, the genetic regulating pathway of seed shattering and abscission layer remains largely unknown.

In present study, we described the cloning and characterization of a novel gene, *SH11*, controlling seed shattering in *O. glaberrima*. *SH11* encodes a MYB transcription factor, which inhibits the expression of genes involved in lignin biosynthesis. Our results indicated that the SNP mutations in the coding region of *SH11* increased the binding ability to the *GH2* promoter and consequently reduced the lignin content in African rice. Knockout of *SH11* significantly reduced seed shattering in *O. glaberrima* using CRISPR-Cas9-mediated approach. These results not only supply new targets for improving seed shattering of African cultivated rice, but also provide novel insights into the molecular mechanism of abscission layer development.

Results

Identification of an introgression line with strong seed shattering

To identify the gene controlling seed shattering difference between *O. glaberrima* and *O. sativa*, we developed a set of introgression lines derived from a cross between *O. sativa* cultivar "Taichung65" (T65) and *O. glaberrima* accession WK21 (accession No. IRGC104038). We obtained one line (GIL292) exhibiting strong seed shattering, which harboured only one WK21 chromosomal segment (Figure S1).

Most seeds of GIL292 shattered by a slight stroke, whereas seeds of T65 remained in the plant (Figure 1a-b). To compare the anatomy of abscission layer between GIL292 and T65, longitudinal sections and fracture surfaces of flower pedicel junction were observed using confocal microscopy and scanning electron microscopy (SEM), respectively. GIL292 exhibited a complete abscission layer between the pedicel and spikelet and a smooth fracture surface (Figure 1c–f), whereas T65 had an intermittently distributed abscission layer and its fracture surface cells displayed a smooth to rough transition from periphery to the centre of transverse plane (Figure 1g–j). These results indicated that the difference in seed shattering in GIL292 and T65 was caused by a different abscission layer structure.

Map-based cloning of *SH11*

Genetic linkage analysis of 107 F_2 individuals derived from a cross between GIL292 and T65 showed that seed shattering phenotype was controlled by a single dominant gene, named as *Seed Shattering 11* (*SH11*), located between molecular markers RM224 and M1 on the long arm of chromosome 11 (Figure 2a). Using 817 $F_{2:3}$ plants, we further delimited *SH11* between the markers RM224 and M3 (Figure 2b-c). In this region, the genomic sequence of Nipponbare was ~129 kb containing 12 annotated genes, while the genomic sequence of *O. glaberrima* IRGC104165 was ~42 kb comprising five annotated genes (*G1*–*G5*) (Figure 2d). Quantitative reverse-transcription PCR (qRT-PCR) analysis indicated that only the *G1* gene was expressed in the abscission zone, suggesting that *G1* might be the gene responsible for the shattering phenotypes of GIL292 (Figure S2a).

To confirm this hypothesis, we generated a construct (p*OgSH11*) containing a ~ 5.6-kb fragment including the entire ORF of *G1*, a 2036-bp 5′-flanking region and a 1083-bp 3′-flanking region of GIL292. We transformed this construct into T65 and obtained eight independent transgenic lines. All the transgenic lines showed easier shedding than T65 and abscission layer similar to GIL292 (Figure 2e–g; Figure S2b).

Meanwhile, a CRISPR-Cas9 vector was constructed and transformed into GIL292 to knockout *SH11*. In the T_0 generation, six different heterozygous transgenic plants were identified by sequence analysis. When these transgenic plants were self-pollinated to generate T_1 generations, two homozygous lines, containing 17-bp (Cas9-1) and 22-bp (Cas9-2) deletions in the first exon, were characterized. Both lines knockout *SH11* showed discontinuous abscission layer and reduced seed shattering compared with GIL292 (Figure 2h–k; Figure S2c). These results further confirmed that *G1* was *SH11*.

Expression pattern of *SH11*

The full-length cDNA of *SH11* in GIL292 was 1149 bp in length, with an ORF of 855 bp, a 165-bp 5′-untranslated region (UTR) and a 129-bp 3′-UTR, and was predicted to be a MYB transcription factor (www.ebi.ac.uk). To examine the subcellular localization of SH11, we constructed *SH11-GFP* and *SH11-RFP* fusion genes under the control of the CaMV35S promoter and co-transformed into rice protoplasts. GFP and RFP fluorescence signals were both detected in nucleus (Figure 3a). Transcriptional activation experiments in yeast indicated that SH11 had transcriptional activity and residues from 133 to 285aa of SH11 were required for its transcriptional activity (Figure S3).

The expression pattern of *SH11* was examined by qRT-PCR. Apart from abscission zone before or after flowering, *SH11* was mainly expressed in culms, leaves and glumes, but rarely in roots and young panicles (Figure 3b). We further explored localization of *SH11* mRNA using in situ hybridization. As shown in Figure 3c, hybridization signal was specifically observed in abscission layer in T65 and GIL292, consistent with its role in seed shattering.

Identification of the causal mutations of *SH11*

In order to determine whether variation in the coding region or the promoter region caused the difference of seed shattering between GIL292 and T65, two chimeric vectors (CV1 and CV2) were developed using the coding sequence of *OgSH11* driven by the promoter of T65 or GIL292, respectively (Figure 4a). Transgenic T65 plants with CV1 or CV2 exhibited easier seed shattering than T65. Furthermore, overexpressing *OgSH11* in T65 increased seed shattering, but overexpressing *OsSH11* did not change the seed shattering in T65 (Figure 4b–e). These results indicated that variation in protein sequences accounted for the different seed shattering between GIL292 and T65.

Moreover, another CRISPR-Cas9 vector was constructed to knockout *OsSH11* and transformed into T65, and we found that two T_1 lines (Cas9-3 and Cas9-4) displayed similar seed shattering with T65 (Figure S4). These results suggested that the *OgSH11* allele gained the new function of controlling seed shattering.

To identify the causal mutations of *SH11* for seed shattering, we compared the coding region sequences of *SH11* between GIL292 and T65 and found 12 SNPs and three insertion/deletions (InDels), which caused six amino-acid changes (Figure S5). We sequenced the *SH11* coding region of 78 African rice accessions: 15 *O. barthii* and 63 *O. glaberrima*. We found that all the *O. barthii* and *O. glaberrima* were clustered into 3 and 18 haplotypes, respectively. The S1 (deletion of CGA) and S2 (insertion of CAG) sites were also shared in all haplotypes (Figure S6). Therefore, we inferred that the mutation of these two sites might be the causal mutations.

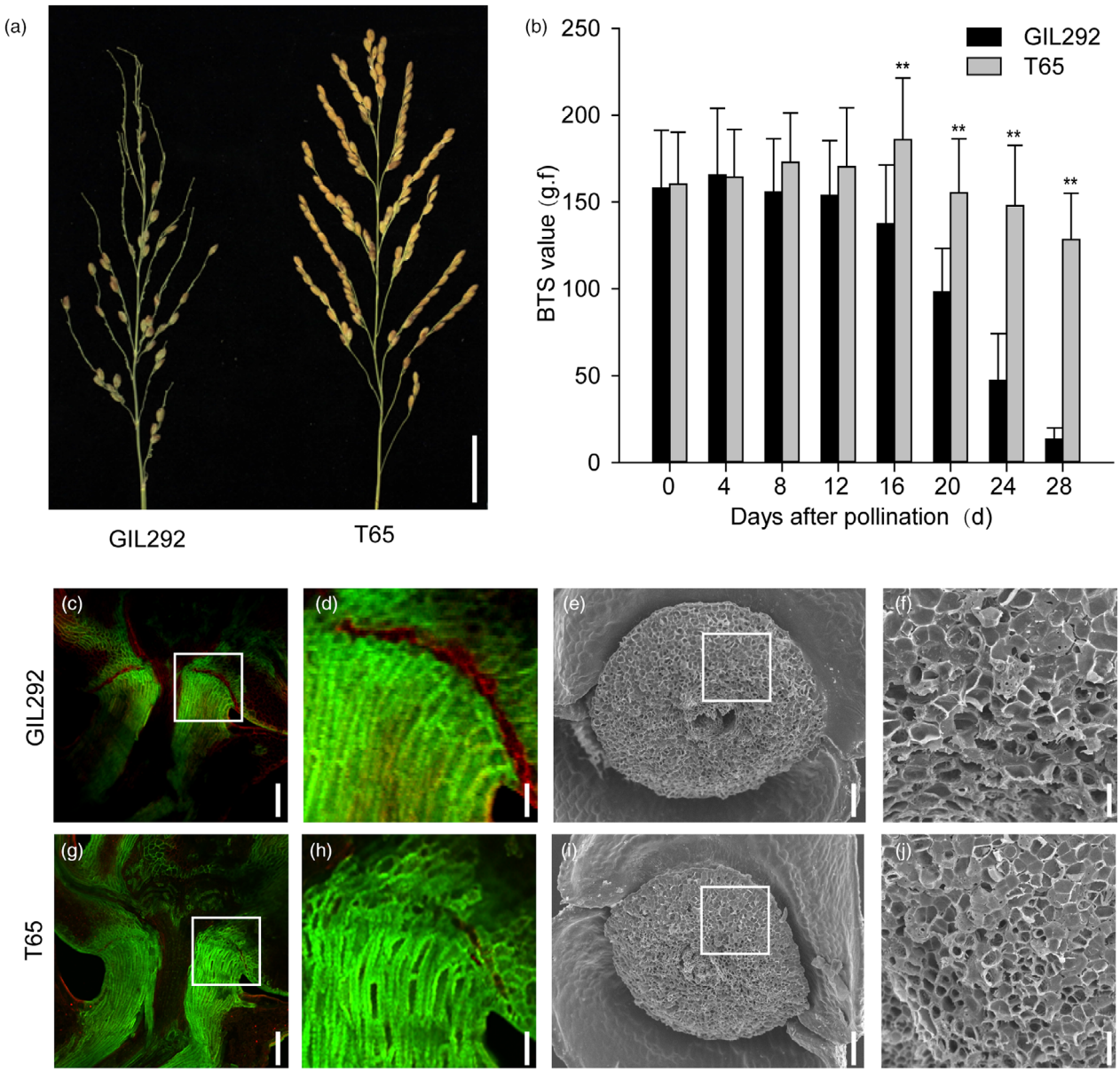

Figure 1 Comparison of seed shattering and floral abscission zone morphologies between GIL292 and T65. (a) Comparison of panicles between GIL292 and T65 at mature stage. Scale bar, 5 cm. (b) Comparison of the BTS value between GIL292 and T65 on the day of pollination and every 4 days, thereafter during seed development. The g.f mean represents gravitational unit of force. Data are presented as mean ± SD ($n = 35$). ** $P < 0.01$, Student's *t* test. (c, g) Fluorescence images of longitudinal sections across grain pedicel junction stained by acridine orange. Scale bars, 100 μm. (d, h) Enlargements of the white boxes in (c) and (g), respectively. Scale bars, 50 μm. (e, i) Scanning electron microscopy (SEM) photographs of pedicel junction after seed detachment. Scale bars, 100 μm. (f, j) Close-up views of white boxes in (e) and (i). Scale bars, 50 μm.

To verify this hypothesis, we generated three site-directed mutagenesis vectors, for introducing S1 or S2 or both mutations of GIL292 into T65 (Figure 4f). Transgenic plants with either S1 or S2 site exhibited similar level of seed shattering to GIL292, confirming that S1 and S2 were the causal mutations responsible for seed shattering in GIL292 (Figure 4g–i).

SH11 regulates seed shattering by affecting lignin biosynthesis

To understand the molecular function of *SH11*, we performed RNA-seq using the abscission zone before flowering of GIL292 and Cas9-1 (knockout of *SH11* in the GIL292 background). A total of 2823 differentially expressed genes (DEGs) were identified, including 1678 up-regulated genes and 1145 down-regulated genes in Cas9-1 compared with GIL292 (fold change ≥ 2, FDR < 0.001).

Previous studies have shown that lignin content plays an important role in seed shattering in rice (Yoon *et al.*, 2014, 2017). Interestingly, we found seven genes involved in lignin biosynthesis up-regulated in Cas9-1 (Figure 5a), and similar expression trends were detected using qRT-PCR (Figure S7) (Hirano *et al.*, 2012; Huang *et al.*, 2018; Li *et al.*, 2003; Sakamoto *et al.*, 2016; Tonnessen *et al.*, 2015).

To test whether *SH11* was related to lignin metabolism, we measured the lignin contents in GIL292 and Cas9-1 and found

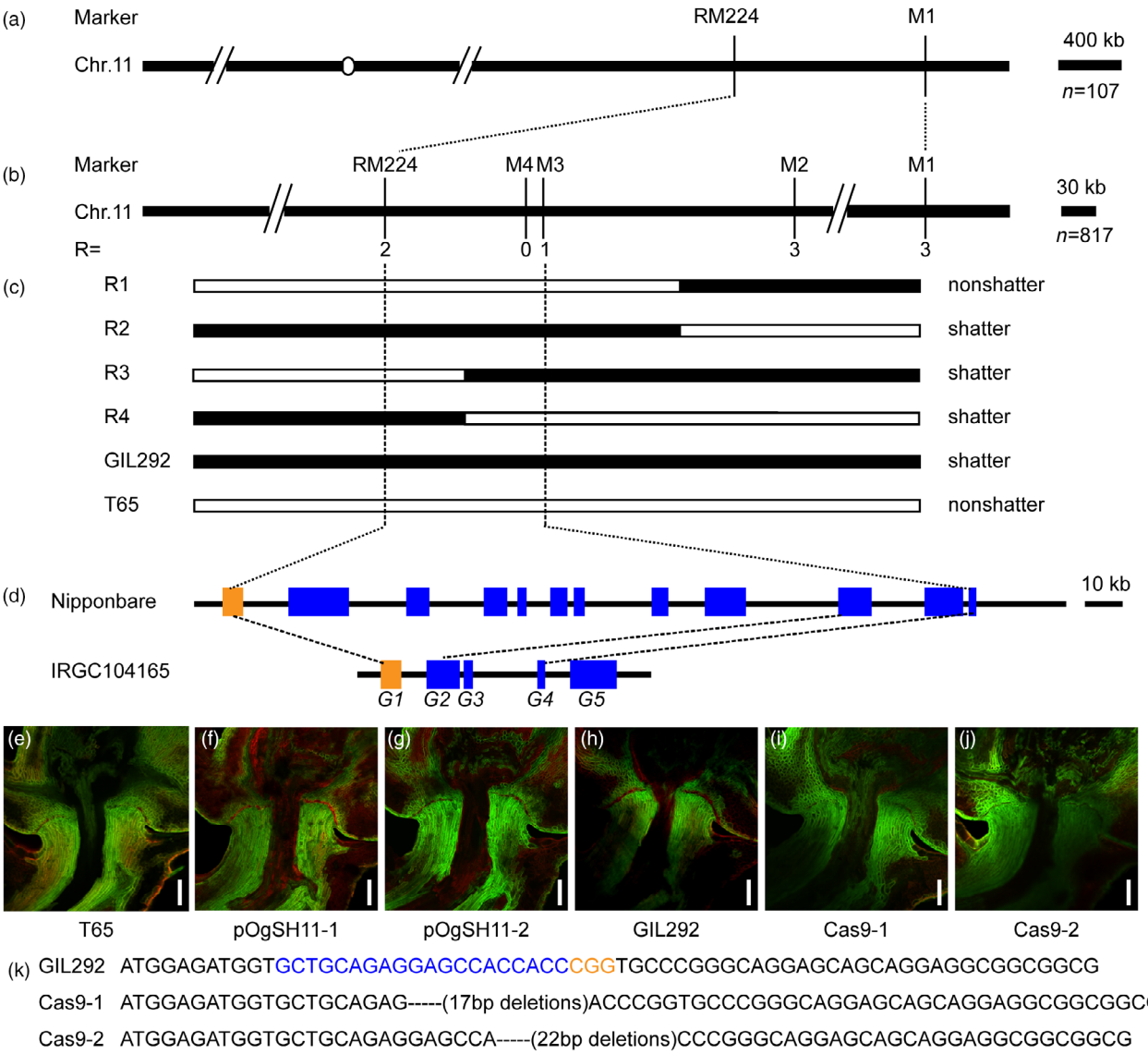

Figure 2 Fine mapping and cloning of *SH11*. (a) The target gene (or genes) for seed shattering was located between RM224 and M1 on the long arm of chromosome 11 based on linkage analysis of 107 F_2 individuals. (b, c) *SH11* was further narrowed down to a region between markers RM224 and M3 using 817 $F_{2:3}$ individuals. (d) Schematic diagrams of comparison of the annotated genes on the genome sequences between Nipponbare and IRGC104165, *G1* is highlighted in orange. (e–g) Fluorescence images of longitudinal sections across grain pedicel junction stained by acridine orange in T65 (e), transgenic line of p*OgSH11*-1 (f) and p*OgSH11*-2 (g), scale bars, 100 μm. (h–j) Fluorescence images of longitudinal sections across grain pedicel junction stained by acridine orange in introgression line GIL292 (h), CRISPR-Cas9 knockout lines Cas9-1 (i) and Cas9-2 (j), scale bars, 100 μm. (k) Sequences of the first exon of the candidate gene in transgenic plants Cas9-1 and Cas9-2, edited using the CRISPR-Cas9 technique, GIL292 as the control. The sgRNA sequence was marked in blue and PAM sequence was marked in orange.

that the level of lignin in abscission zone of Cas9-1 was significantly higher than that of GIL292 (Figure 5b). Meanwhile, staining using lignin-specific dye showed darker stain indicating higher lignin deposition in Cas9-1 (Figure 5c-d). These results suggested that *SH11* might suppress lignin deposition in the side of abscission layer.

SH11 regulates seed shattering by directly binding the promoter of *GH2*

Previous studies indicated that cinnamyl-alcohol dehydrogenase functions in the last step of lignin monomer biosynthesis, converting hydroxyl-cinnamaldehydes into their corresponding alcohols, and the expression of *GH2* was the most abundant (Hirano *et al*., 2012). In addition, *GH2* was reported to be highly correlated to seed shattering (Jiang *et al*., 2019; Yoon *et al*., 2014, 2017). As was mentioned above, the result of qRT-PCR indicated that *OgSH11* negatively regulates the expression of *GH2* (Figure S7). In addition, we overexpressed the *GH2* gene in GIL292. The transgenic plants that overexpressing *GH2* decreased seed shattering through altering the abscission layer development (Figure 6a–d; Figure S8a).

To determine whether OgSH11 directly binds to *GH2* promoter, the promoter of *GH2* was divided into eight fragments and inserted into placZi vector, respectively. Binding signal was

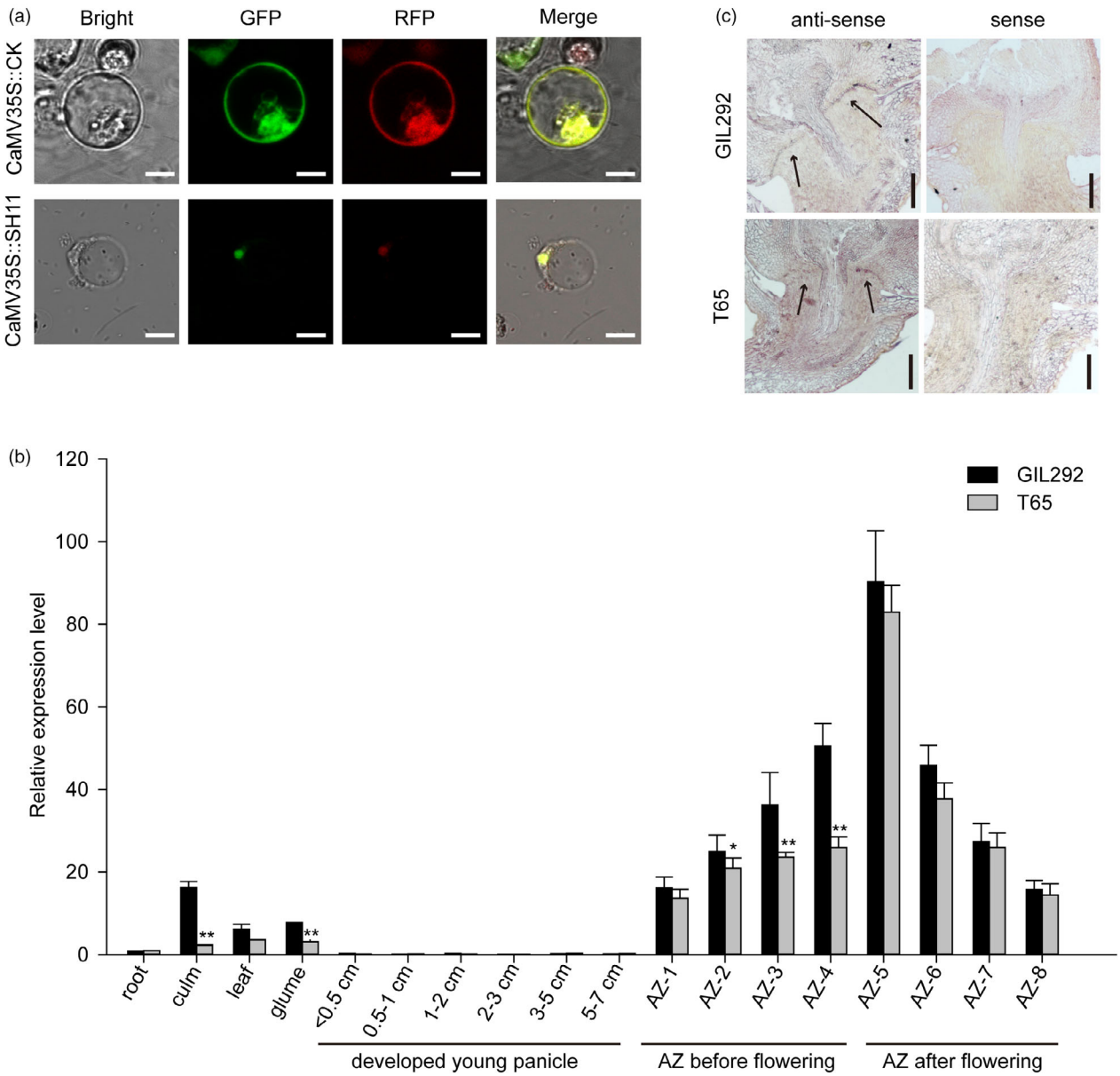

Figure 3 Expression pattern of *SH11*. (a) The CAMV35Spro::GFP, CAMV35Spro::RFP, CAMV35Spro::SH11-GFP and CAMV35Spro::SH11-RFP fusion were expressed transiently in rice protoplast. Bright, bright-field image; GFP, the GFP channel; RFP, the RFP channel; Merge, all channels merged. Scale bars, 200 μm. (b) Expression pattern of *SH11* in GIL292 and T65 are presented as mean ± SD. ($n = 3$). *$P < 0.05$, **$P < 0.01$, Student's *t* test. AZ-1 to AZ-4 correspond to stage sp6, sp7, 2 days after sp7 and sp8, respectively. AZ-5 to AZ-8 correspond to 0, 4, 8, 12 days after flowering, respectively. AZ is short for abscission zone. (c) mRNA in situ hybridization of *SH11* at stage sp8 (formation of ovule and pollen). Arrows indicate the abscission layer. Scale bars, 100 μm.

detected in the region of −123 ~ −359 using the yeast one-hybrid system (Figure S8b). We then searched for transcription factor–binding sites in this region using the online software New PLACE and PlantPAN3.0 (Chow *et al.*, 2019; Higo *et al.*, 1999) and found a *cis* element (ACCAACC) targeted by MYB transcription factors in this region. Once this *cis* element was removed from this region, colour of yeast colonies and β-galactosidase activity were reduced compared with yeast transformed with wild-type sequences and OgSH11 and OsSH11 (Figure 6e-f; Figure S8c). Moreover, Electrophoretic Mobility Shift Assay (EMSA) using His-OgSH11 and His-OsSH11 recombinant protein showed that OgSH11 had a stronger binding activity although both SH11 recombinant proteins could bind to *GH2* promoter (Figure 6g).

Taken together, all these results indicated that *SH11* regulated seed shattering via binding the promoter of *GH2* directly and suppressed its expression in African cultivated rice.

Editing *SH11* improved seed shattering in *O. glaberrima*

To further explore the application potential of *SH11* in African rice breeding, we introduced a CRISPR-Cas9 construct into WK21, an endemic accession of *O. glaberrima*, and regenerated four T_0 transgenic plants. In the T_1 generations, two homozygous knockout lines (Cas9-5 and Cas9-6) containing a 4-bp and a

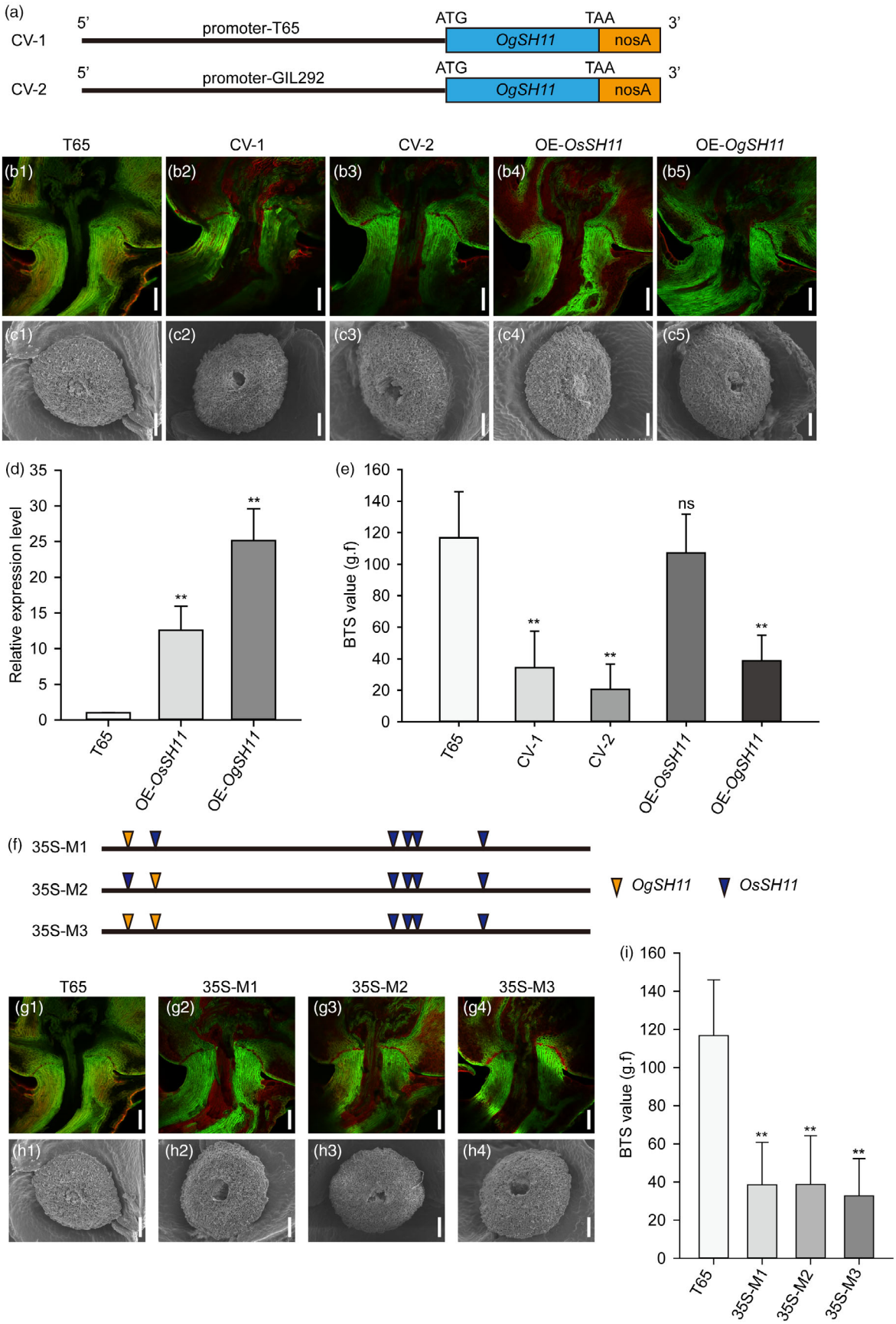
(a)
CV-1
5'
promoter-T65
ATG
TAA
3'
OgSH11
nosA
CV-2
5'
promoter-GIL292
ATG
TAA
3'
OgSH11
nosA
T65
CV-1
CV-2
OE-OsSH11
OE-OgSH11
(b1)
(b2)
(b3)
(b4)
(b5)
(c1)
(c2)
(c3)
(c4)
(c5)
(d)
Relative expression level
T65
OE-OsSH11
OE-OgSH11
(e)
BTS value (g.f)
ns
T65
CV-1
CV-2
OE-OsSH11
OE-OgSH11
(f)
35S-M1
35S-M2
35S-M3
OgSH11
OsSH11
T65
35S-M1
35S-M2
35S-M3
(g1)
(g2)
(g3)
(g4)
(h1)
(h2)
(h3)
(h4)
(i)
BTS value (g.f)
T65
35S-M1
35S-M2
35S-M3

Figure 4 Causal mutations analysis of *SH11*. (a) Schematic diagrams of two chimeric vectors. CV, chimeric vector. (b) Fluorescence images of longitudinal sections across flower pedicel junction stained by acridine orange in T65(b1), CV-1(b2), CV-2(b3), OE-*OsSH11*(b4) and OE-*OgSH11*(b5), respectively. Scale bars, 100 μm. (c) SEM photographs of the junction after seeds were detached. T65(c1), CV-1(c2), CV-2(c3), OE-*OsSH11*(c4) and OE-*OgSH11*(c5), respectively. Scale bars, 100 μm. (d) qRT-PCR of *SH11* in T65, OE-*OsSH11* and OE-*OgSH11*. Data are presented as mean ± SD ($n = 3$). $^{**}P < 0.01$, Student's *t* test. (e) Comparison of the BTS value at day 28 days after pollination in T65, CV-1, CV-2, OE-*OsSH11* and OE-*OgSH11*. The g.f represents gravitational unit of force. Data are presented means ± SD ($n = 35$). ns, no significant, $^{**}P < 0.01$, Student's *t* test. (f) Schematic diagrams of three site-directed mutation vectors. (g) Fluorescence images of longitudinal sections across flower pedicel junction stained by acridine orange in T65 (g1), 35 S-M1 (g2), 35 S-M2(g3) and 35 S-M3(g4), respectively. Scale bars, 100 μm. (h) SEM photographs of the junction after the seeds were detached in T65(h1), 35 S-M1(h2), 35 S-M2(h3), and 35 S-M3(h4), respectively. Scale bars, 100 μm. (i) Comparison of the BTS value at 28 days after pollination in T65, 35 S-M1, 35 S-M2 and 35 S-M3. The g.f represents the gravitational unit of force. Data are presented as mean ± SD ($n = 35$). $^{**}P < 0.01$, Student's *t* test.

25-bp deletion were selected, respectively (Figure 7a). The knockout lines exhibited uncompleted abscission layer and less seed shattering than WK21 (Figure 7b–e; Figure S9). These results demonstrated that knockout of *SH11* in *O. glaberrima* could improve its seed shattering and consequently decrease the loss of harvest.

Discussion

Independent domestication of the two cultivated rice *O. sativa* and *O. glaberrima* not only provides opportunity to understand parallel evolution but also offers resources to improve each other. In this study, we cloned *SH11*, which controls seed shattering in *O. glaberrima*. *SH11* inhibits transcription of *GH2* involved in lignin biosynthesis by directly binding to its promoter. We successfully developed a new *O. glaberrima* material showing significantly reduced seed shattering by targeted mutagenesis of *SH11* in *O. glaberrima* using CRISPR-Cas9-mediated approach. Our results not only supply a new target for improving the seed shattering of African cultivated rice but also provide new insights into the regulatory pathway of abscission layer development.

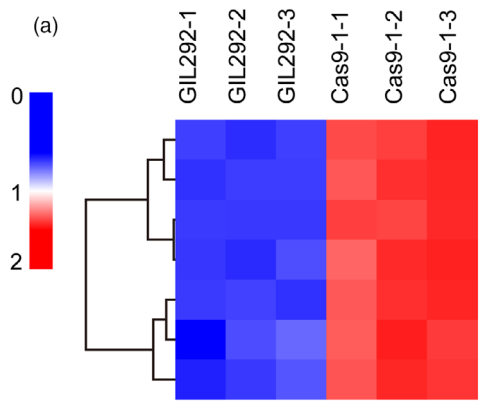

		FPKM		FDR
		GIL292	Cas9-1	
LOC_Os02g09490	*GH2*	47.549	128.727	7.79003E-05
LOC_Os02g41650	*OsPAL2*	149.752	550.322	5.76822E-06
LOC_Os02g41680	*OsPAL4*	45.292	136.295	6.5528E-07
LOC_Os03g30250	*BC1*	3.258	11.511	2.44594E-05
LOC_Os06g04090	*OsSWN1*	2.274	7.187	9.45167E-05
LOC_Os08g06100	*OsCOMT*	78.693	362.896	3.35782E-05
LOC_Os10g29470	*OsCAD3*	6.810	19.391	1.06829E-05

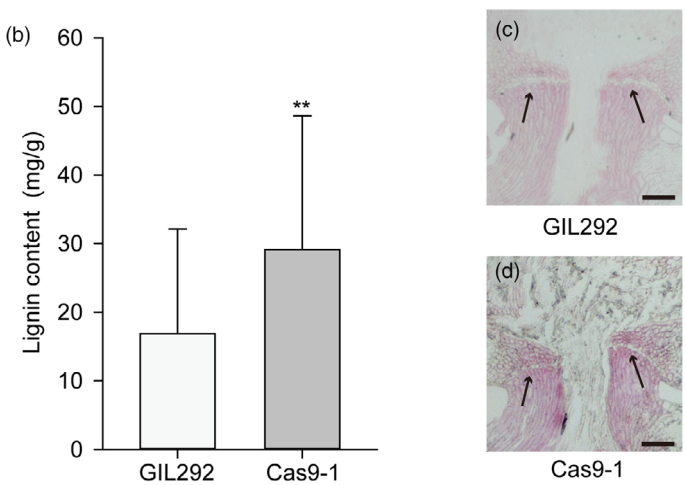

Figure 5 *SH11* inhibits biosynthesis of lignin. (a) Hierarchical clustering of 7 DEGs involved in lignin biosynthesis in three biological replicates, data are presented as Z-score. Panel on the right displays average expression levels in FPKM (fragments per kilo-base of exon per million mapped reads) and FDR (False Discovery Rate). (b) Comparison of lignin content of AZ at mature stage between GIL292 and Cas9-1. Data are presented as mean ± SD ($n = 3$). $^{**}P < 0.01$, Student's *t* test. AZ is short for abscission zone. (c, d) Comparison of lignin deposition in the pedicel junction at spikelet developmental stage sp8, stained with 1% (w/v) phloroglucinol. Arrows indicate the abscission layer.

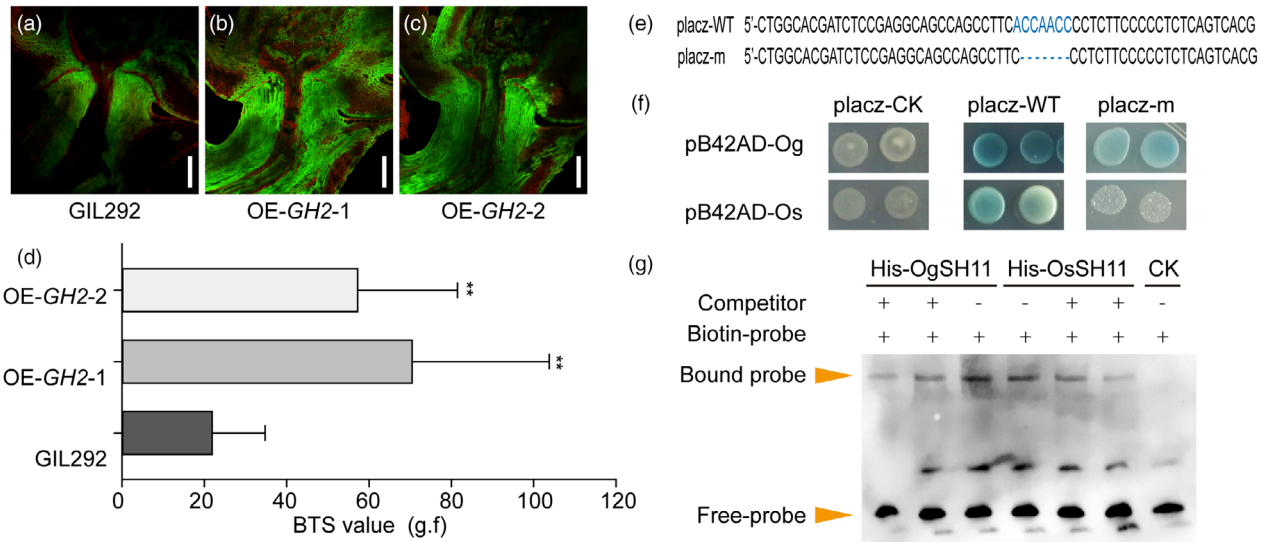

Figure 6 *SH11* affects lignin biosynthesis via binding *GH2* promoter. (a–c) Fluorescence images of longitudinal sections across flower pedicel junction stained by acridine orange in GIL292 (a), OE-*GH2*-1 (b) and OE-*GH2*-2 (c), respectively. Scale bars, 100 μm. (d) Comparison of the BTS value at 28 days after pollination in GIL292, OE-*GH2*-1 and OE-*GH2*-2. The g.f represents the gravitational unit of force. Data are presented as mean ± SD (n = 35). **P < 0.01, Student's t test. (e) The region tested for binding of SH11 in the *GH2* promoter. (f) Yeast one-hybrid analysis of OgSH11 and OsSH11 binding to *GH2*. The promoter sequences were fused with *lacZ* reporter and the blue colonies indicated interaction between SH11 and promoter. (g) EMSA revealed that both His-OgSH11 and His-OsSH11 were able to bind to the *GH2* promoter, and His-OgSH11 showed higher affinity.

SH11 provides a new target for improvement of African cultivated rice

Loss of seed shattering is one of the key steps during the domestication of *O. sativa*. However, superior climate in ancient African means there was an abundant of food, making efficient cereal production less critical (Champion *et al.*, 2021; Hoag and Svenning, 2017). Crops that are being domesticated were frequently neglected; as a result, these crops remained some degree of seed shattering to reproduce by themselves, and this is likely the reason why *O. glaberrima* still exhibits relatively high degree of seed shattering nowadays, despite that it has been selected for reduced shattering at *SH3* or *GL4* locus (Lv *et al.*, 2018; Wu *et al.*, 2017).

However, with increases in populations and changes in the natural environment, selection of only major genes could no longer meet the needs of crop production. Compared with Asian cultivated rice, strong seed shattering of African cultivated rice represents a key factor of its harvest loss. On the other hand, planting Asian cultivated rice can improve yields, although the adaption to local environments and the high cost of production are also great challenges.

Our present work indicates that *SH11* encodes a MYB transcription factor, inhibits lignin biosynthesis and reduces lignin deposition via transcriptional repression of *GH2*, a key enzyme involved in lignin monomer biosynthesis. In particular, *SH11* affects seed shattering via modulating the lignin deposition at the side of abscission layer. The plant of knockout *SH11* exhibited significantly reduced seed shattering in *O. glaberrima*, indicating that *SH11* is a brilliant target for improving seed shattering in *O. glaberrima*.

Regulation of the cellulose and lignin biosynthesis is critical by different transcription factors controlling seed shattering

Seed shattering is an important trait for rice domestication and improvement. The main structure of seed shattering in rice is the abscission layer, whose development and degradation are closely relative to shedding traits. Previous studies have identified several genetic factors controlling seed shattering in rice, such as *qSH1*, *SH4/SHA1*, *SHAT1*, *SH3*, *SH5* and *SSH1* (Jiang *et al.*, 2019; Konishi *et al.*, 2006; Li *et al.*, 2006; Lin *et al.*, 2007; Lv *et al.*, 2018; Win *et al.*, 2017; Wu *et al.*, 2017; Yoon *et al.*, 2014; Zhou *et al.*, 2012). Most of these are transcription factors, which perform important roles in the development of abscission layer.

It is well-known that cellulose and lignin are important components of cell walls, whose content makes great influences on the structure and function of the cell well. Both *SH4* and *SH11* are MYB transcription factors. In this study, we found that *OgSH11* represses the expression of lignin biosynthesis genes, and the mutant of *SH11* showed higher lignin content than the wild type (Figure 5). In order to determine the biotech function of *SH4*, we generated a *sh4* mutant using CRISPR-Cas9 technique in the background of T65 and performed RNA-seq using abscission zones from them. Interestingly, we found that *sh4* mutant reduced the expression level of genes related to cellulose synthesis (Figure S10), which suggested that *SH4* controls seed shattering through controlling cellulose synthesis. These results demonstrated that different MYB transcription factors regulate seed shattering through different pathways.

In addition, several genes controlling seed shattering, such as *qSH1*, *SH5*, *SSH1* and *OSH15*, made an influence on lignin biosynthesis by inhibiting the expression of *GH2* (Jiang *et al.*, 2019; Yoon *et al.*, 2014, 2017). In the present study, we found that *SH11* can directly bind to the promoter of *GH2* and inhibit its expression, leading to an easy-shattering phenotype in African cultivated rice.

The *OgSH11* gained new function of regulating seed shattering before the domestication of wild rice to cultivated rice

Asian cultivated rice (*O. sativa*) and African cultivated rice (*O. glaberrima*) were independently domesticated from the wild progenitor species *O. rufipogon* and *O. barthii*, respectively. The two wild

(a) WK21 GCAGAGGAGCCACCACCCGGTGCCCGGGCAGGAGCAGCAGGAGGCGGCGGCGGAGCTGTCGTCGGC
TGAGCTCCGGCGAGGGCCATGGACCGTCGACGAGGACCTCACCCTCA

Cas9-5 GCAGAGGAGCCACCACCCGGTGCCCGGGCAGGAGCAGCAGGAGGCGGCGGCGGAGCTGTCGTCGGC
TGAGCTCCGGCGAGGGCCATGGACCGTCGACGAGGACCT----(4bp deletions)CTCA

Cas9-6 GCAGAGGAGC----------(25bp deletions)AGCAGGAGGCGGCGGCGGAGCTGTCGTCGGC
TGAGCTCCGGCGAGGGCCATGGACCGTCGACGAGGACCTCACCCTCA

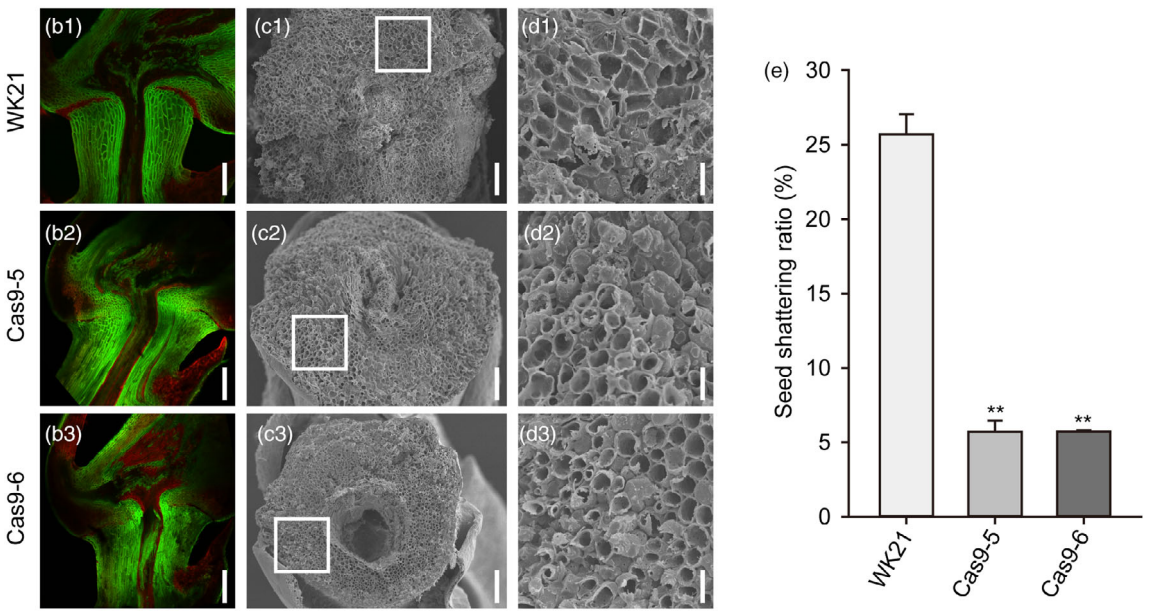

Figure 7 Use of *SH11* to reduce seed shattering in *O. glaberrima*. (a) Sequence of the first exon of *SH11* in transgenic plants, which were edited using CRISPR-Cas9 technique, WK21 as the control. The sgRNA sequence was marked in blue and PAM sequence was marked in orange. (b) Fluorescence images of longitudinal sections across flower pedicel junction stained by acridine orange in WK21 (b1), Cas9-5 (b2) and Cas9-6 (b3). Scale bars, 100 μm. (c) SEM photographs of the junction after detachment of seeds in WK21 (c1), Cas9-5 (c2) and Cas9-6 (c3). Scale bars, 100 μm. (d) Close-up views of the white boxes in (c1), (c2) and (c3), respectively. Scale bars, 50 μm. (e) Comparison of the seed shattering ratio of WK21, Cas9-5 and Cas9-6. Values are means ± SD ($n = 5$). $^{**}P < 0.01$, Student's *t* test.

progenitor species divergence occurred about 0.6 million years ago (Purugganan, 2014). Great genomic sequences differences have been accumulated during the evolution of the two species. In fact, the genome of *O. glaberrima* is about 345-Mb, which is smaller than that of *O. sativa* (Shang *et al.*, 2022). Abundant phenotypic differences also accumulated between the two cultivated rice species to fit different environment and human demands. However, the genetic basis responsible for the phenotypic differences between the two cultivated species remains largely unknown.

In this study, we identified a novel gene, *SH11*, controlling seed shattering in African rice. Interestingly, the homologous gene of *SH11* in Asian rice does not control seed shattering. The S1 and S2 were the causal mutations responsible for seed shattering in African cultivated rice. The African cultivated rice and its progenitor *O. barthii* shared the same haplotype on these two mutation sites. The Asian cultivated rice and its progenitor *O. rufipogon* shared another haplotype on these two mutation sites (Figure S11). These results demonstrated that the differentiation of *SH11* occurred before the domestication of wild rice to cultivated rice.

Experimental procedures

Plant materials and growth conditions

For the map-based cloning of *SH11*, expression pattern analysis and genetic transformation, Taichuang65 (T65) and GIL292 were used. T65 is an Asian cultivated rice accession (*O. sativa*), collected from Taiwan province, China. GIL292 is an introgression line derived from the cross between T65 and WK21 (IRGC101435, *O. glaberrima*). The F_2 segregating population was derived from the cross between T65 and GIL292. Other cultivars and wild-rice accessions are listed in Table S1. All plants were grown in the field conditions in Beijing (May–October) or Hainan province (November–April the next year), China.

Evaluation of seed shattering

The degree of shattering was measured 28 days after pollination with a slight stroke by hand. Plants with >80% seeds removed from the panicle were identified shattering. For BTS, a total of 35 grains from the panicles were measured with a digital force gauge (FGP-1; SHIMPO), and the maximum tensile strength was recorded until the grain was pulled off from the pedicel (Units: gram-force (g.f)).

Primers and probes

The primers and probes used in this study are listed in Table S2.

Histological analysis and SEM

To observe the AZ structure, abscission layers on the flowering day were selected and longitudinally sectioned by hand. The sections were submerged in 0.01% (w/v) acridine orange for

several minutes (Briggs and Morris, 2008) and flushed three times using deionized water. The tissues were observed with 488-nm excitation and a 543-nm emission wavelengths using a Leica SP8 laser scanning microscope. To examine lignin deposition, AZ before heading were collected from GIL292 and Cas9-1, processed as described by Yoon *et al*. (2014) and were stained with phloroglucinol in 20% (v/v) HCl. For scanning electron microscopy, the pedicel junctions after detachment of mature seeds and the second last internodes after rice filling were gold plated and observed under a Hitachi S-2460 scanning electron microscope.

Fine mapping of *SH11*

F_2 and $F_{2:3}$ populations were derived from the cross between Taichung 65 and GIL292. DNA was extracted from fresh leaves using the cetyl-trimethyl-ammonium bromide method (Murray and Thompson, 1980). The detail information of the primers used in this study is displayed in the Table S2.

Generation of constructs and transformation

Constructs for CRISPR-Cas9-based genome editing of *SH11* were performed as previously described (Ma *et al*., 2015). The functional complementary construct was prepared by inserting the ~5.7-kb genomic fragment encompassing the entire *OgSH11* gene into the binary vector pCAMBIA1300 between *Kpn* I and *Xba* I sites. For overexpression, African cultivar and Asian cultivar type *SH11* open reading frame were amplified using the primer OE-SH11-F and OE-SH11-R and cloned into the binary vector pCAMBIA1301 (http://www.cambia.org) between the *BamH* I and *Spe* I sites under control of CaMV35S promoter. The chimeric vectors were made by linking ~2.5-kb promoter fragments of *OgSH11* or *OsSH11* to African cultivar type *SH11* open reading frame. The construct p*35S::SH11-GFP* and p*35S::SH11-RFP* contained the SH11 coding region except the TAA stop codon were removed and fused with *GFP* and *RFP*, respectively, under control of CAMV35S promoter. All constructs were introduced into *Agrobacterium tumefaciens* strain EHA105. *Agrobacterium*-mediated transformation was performed by Biorun Biosciences Co., Ltd, Wuhan, China.

Subcellular localization

To determine the subcellular localization of SH11, two plasmids were generated: p*35S::SH11-RFP* and p*35S::SH11-GFP*. The two plasmid constructs were co-transformed into rice protoplasts as described by Bart *et al*. (2006). After 12 h incubation at 28 °C in the dark, GFP and RFP fluorescence were examined with excitation of 488-nm and emission of 543-nm wavelength under a Leica SP8 laser scanning microscope.

RNA extraction, RACE and RT-PCR

Total RNAs used for RACE and RNA-seq were extracted using Trizol reagent (Thermo Fisher Scientific) and purified using the RNAclean Kit (Aidlab Biotechnologies). Total RNAs used for RT-PCR were extracted using EASYspin Kit (Aidlab Biotechnologies), following manufacturer's instructions. First-strand cDNA was synthesized using M5 Super qPCR RT Kit with gDNA remover (Mei5bio). The 5′- and 3′- RACE were conducted with SMARTer RACE 5′/3′ kit (TaKaRa) following manufacturer's instructions. Real-time PCR was performed using a CFX96 real-time system (Bio-Rad) and Hiper SYBR Premix Es Taq (Mei5bio). Three replicates were performed and rice *ACTIN1* was used as the internal control (Livak and Schmittgen, 2001). Primers used for qRT-PCR are listed in Table S2.

RNA in situ hybridization

Abscission zones before flowering were collected from Taichung 65 and GIL292 and fixed in 3.7% (v/v) Formalin-Acetic Acid-Alcohol solution, then subjected to a series of dehydration and infiltration and embedded in paraffin. The tissues were sectioned into 10-μm sections using a microtome (Leica RM2145). A 253-bp fragment of *SH11* cDNA was amplified and used as templates to generate sense and anti-sense digoxigenin-labelled RNA probes, which were prepared using a DIG RNA labelling kit (Roche, Shanghai, China). The mRNA hybridization and immunological detection of the hybridized probes were performed as described previously (Zhang *et al*., 2007).

Transcriptional activity assay

The vectors and yeast strains (Matchmaker GAL4 Two-Hybrid System 3) were obtained from Clontech, Beijing, China. The Y2H assay was performed according to the manufacturer's instructions (Takara). After 3 days of incubation at 30 °C, single yeast colonies were spotted on selection plates. Several clones were selected into new media for further screening of nutritional defects.

RNA-seq analysis

Total RNA was isolated from abscission zones before flowering of GIL292 and Cas9-1, with three biological replicates and three plants in each replicate, abscission zones before flowering of T65 and *sh4* mutant, with two biological replicates and three plants in each replicate. Paired-end libraries were constructed and sequenced using an Illumina HiSwq2500 at Biomarker Technologies Co., Ltd., China. The raw reads were mapped to the reference genome (Os-Nipponbare-Reference-IRGSP-1.0, MSU7) using TopHat2 with default parameters (Kim *et al*., 2013), and differentially expressed genes (DEGs) (fold change ≥2, FDR <0.01) (Trapnell *et al*., 2010) between GIL292 and Cas9-1 were determined using BMKCloud.

Evaluation of lignin content

After rice filling, the second last internodes were selected and dried at 80 °C for more than 3 days, and the lignin content was determined using lignin content detection kit (BC4200, Solarbio, Beijing, China) according to the manufacturer's instructions.

Yeast one-hybrid assays

The AD fusions were co-transformed into the yeast strain EGY48, with the *LacZ* reporter gene driven by various *GH2* promoter fragments and spread on SD/−Trp/-Ura medium. After 3 days of incubation at 30 °C, positive clones were transferred to SD/−Trp/-Ura medium with X-Gal for blue colour development. Relative β-galactosidase activity was quantified by hydrolysis of *o*-nitrophenyl-β-D-galactopyranoside (N1127, Sigma, Shanghai, China). The absorbance for the released *o*-nitrophenyl compound was measured on a spectrophotometer at 420-nm.

Protein expression and EMSA

Recombinant His-OgSH11 and His-OsSH11 were expressed in *Escherichia coli* Rosetta (DE3) and purified by M5 Ni-Agarose His-Tagged Protein Purification Kit (soluble protein) (Mei5bio, MF207). Before EMSA, His-OgSH11 and His-OsSH11 were normalized in the same concentration. The EMSA was done using LightShift™ Chemiluminescent EMSA Kit (20148, Thermo Scientific™, Shanghai, China) according to its instructions. The biotin-labelled DNA fragments listed in Table S2 are synthesized

by Tsingke Biotechnology Co., Ltd, Beijing, China. and used as probes; unlabelled DNA fragments of the same sequences were used as the competitors.

Sequencing and data analysis

The ~3.3-kb genomic fragment covering the harbouring *SH11* gene (2491 bp), the 436 bp 5′-flanking region and the 403 bp 3′-flanking region were amplified using four pairs of PCR primers and sequenced using Sanger sequencing approach. Sequences were assembled via ContigExpress Project. Multiple sequences were aligned with DNAMAN.

Acknowledgements

We thank Prof. Yaoguang Liu (South China Agricultural University) for providing pYLCRISPR/Cas9Pubi-H vector. We thank the International Rice Research Institute, the Japan National Institute of Genetics and the United States Department of Agriculture-Agricultural Research Service for providing the wild rice and cultivated rice samples. This research was supported by the National Natural Science Foundation of China (Grant No. 31925029 and 32261143756) and Hainan Yazhou Bay Seed Lab (Grant No. B21HJ0111). The funders had no role in study design, data collection and analysis, decision to publish or preparation of the manuscript.

Conflict of interest

The authors declare they have no conflict of interest.

Author contributions

Z. Z. designed and supervised this study. J. N. performed most of the experiments. W.H., L. W., M. H. and L. C. performed evolutionary analysis of *SH11*. Y. F., H. S., F. L., P. G. and C.S. collected rice germplasm. Z. Z., J. N. and N.M. wrote the manuscript.

REFERENCES

Bart, R., Chern, M., Park, C.J., Bartley, L. and Ronald, P.C. (2006) A novel system for gene silencing using siRNAs in rice leaf and stem-derived protoplasts. *Plant Methods*, **2**, 13.

Briggs, C.L. and Morris, E.C. (2008) Seed-coat dormancy in *Grevillea linearifolia*: little change in permeability to an apoplastic tracer after treatment with smoke and heat. *Ann. Bot.* **101**, 623–632.

Champion, L., Fuller, D.Q., Ozainne, S., Huysecom, E. and Mayor, A. (2021) Agricultural diversification in West Africa: an archaeobotanical study of the site of Sadia (Dogon Country, Mali). *Archaeol. Anthropol. Sci.* **13**, 60.

Chow, C.N., Lee, T.Y., Hung, Y.C., Li, G.Z., Tseng, K.C., Liu, Y.H., Kuo, P.L. *et al*. (2019) PlantPAN3.0: a new and updated resource for reconstructing transcriptional regulatory networks from ChIP-seq experiments in plants. *Nucleic Acids Res.* **47**, D1155–D1163.

FAO. (2021) *Hunger and food insecurity*. http//www.fao.org/hunger/en/

Higo, K., Ugawa, Y., Iwamoto, M. and Korenaga, T. (1999) Plant cis-acting regulatory DNA elements (PLACE) database. *Nucleic Acids Res.* **27**, 297–300.

Hirano, K., Aya, K., Kondo, M., Okuno, A., Morinaka, Y. and Matsuoka, M. (2012) *OsCAD2* is the major *CAD* gene responsible for monolignol biosynthesis in rice culm. *Plant Cell Rep.* **31**, 91–101.

Hoag, C. and Svenning, J.-C. (2017) African environmental change from the Pleistocene to the Anthropocene. *Annu. Rev. Env. Resour.* **42**, 27–54.

Huang, P., Yoshida, H., Yano, K., Kinoshita, S., Kawai, K., Koketsu, E., Hattori, M. *et al*. (2018) *OsIDD2*, a zinc finger and INDETERMINATE DOMAIN protein, regulates secondary cell wall formation. *J. Integr. Plant Biol.* **60**, 130–143.

Ji, H., Kim, S.R., Kim, Y.H., Kim, H., Eun, M.Y., Jin, I.D., Cha, Y.S. *et al*. (2010) Inactivation of the CTD phosphatase-like gene *OsCPL1* enhances the development of the abscission layer and seed shattering in rice. *Plant J.* **61**, 96–106.

Jiang, L., Ma, X., Zhao, S., Tang, Y., Liu, F., Gu, P., Fu, Y. *et al*. (2019) The APETALA2-Like transcription factor *SUPERNUMERARY BRACT* controls rice seed shattering and seed size. *Plant Cell*, **31**, 17–36.

Jones, M.P., Dingkuhn, M., Aluko, G.K. and Semon, M. (1997) Interspecific *Oryza sativa* and *O. glaberrima* progenies in upland rice improvement. *Euphytica*, **92**, 237–246.

Kim, D., Pertea, G., Trapnell, C., Pimentel, H., Kelley, R. and Salzberg, S.L. (2013) TopHat2: accurate alignment of transcriptomes in the presence of insertions, deletions and gene fusions. *Genome Biol.* **14**, R36.

Konishi, S., Izawa, T., Lin, S.Y., Ebana, K., Fukuta, Y., Sasaki, T. and Yano, M. (2006) An SNP caused loss of seed shattering during rice domestication. *Science*, **312**, 1392–1396.

Li, C.B., Zhou, A.L. and Sang, T. (2006) Rice domestication by reducing shattering. *Science*, **311**, 1936–1939.

Li, X.M., Chao, D.Y., Wu, Y., Huang, X., Chen, K., Cui, L.G., Su, L. *et al*. (2015) Natural alleles of a proteasome alpha2 subunit gene contribute to thermotolerance and adaptation of African rice. *Nat. Genet.* **47**, 827–833.

Li, Y., Qian, Q., Zhou, Y., Yan, M., Sun, L., Zhang, M., Fu, Z., *et al*. (2003) *BRITTLE CULM1*, which encodes a COBRA-like protein, affects the mechanical properties of rice plants. *Plant Cell*, **15**, 2020–2031.

Lin, Z., Griffith, M.E., Li, X., Zhu, Z., Tan, L., Fu, Y., Zhang, W. *et al*. (2007) Origin of seed shattering in rice (*Oryza sativa* L.). *Planta*, **226**, 11–20.

Linares, O.F. (2002) African rice, history and future potential. *Proc. Natl. Acad. Sci. U. S. A.* **99**, 16360–16365.

Livak, K.J. and Schmittgen, T.D. (2001) Analysis of relative gene expression data using real-time quantitative PCR and the $2^{-\Delta\Delta Ct}$ Method. *Methods*, **25**, 402–408.

Lv, S., Wu, W., Wang, M., Meyer, R.S., Ndjiondjop, M.N., Tan, L., Zhou, H. *et al*. (2018) Genetic control of seed shattering during African rice domestication. *Nat. Plants*, **4**, 331–337.

Ma, X., Zhang, Q., Zhu, Q., Liu, W., Chen, Y., Qiu, R., Wang, B. *et al*. (2015) A robust CRISPR/Cas9 system for convenient, high-efficiency multiplex genome editing in monocot and dicot plants. *Mol. Plant*, **8**, 1274–1284.

Meyer, R.S., Choi, J.Y., Sanches, M., Plessis, A., Flowers, J.M., Amas, J., Dorph, K. *et al*. (2016) Domestication history and geographical adaptation inferred from a SNP map of African rice. *Nat. Genet.* **48**, 1083–1088.

Montcho, D., Futakuchi, K., Agbangla, C., Fofana, M. and Dieng, I. (2013) Yield loss of *Oryza glaberrima* caused by grain shattering under rainfed upland conditions. *Int. J. Biol. Chem. Sci.* **7**, 535–543.

Murray, M.G. and Thompson, W.F. (1980) Rapid isolation of high molecular weight plant DNA. *Nucleic Acids Res.* **8**, 4321–4325.

Purugganan, M.D. (2014) An evolutionary genomic tale of two rice species. *Nat. Genet.* **46**, 931–932.

Sakamoto, S., Takata, N., Oshima, Y., Yoshida, K., Taniguchi, T. and Mitsuda, N. (2016) Wood reinforcement of poplar by rice NAC transcription factor. *Sci. Rep.* **6**, 19925.

Shang, L., Li, X., He, H., Yuan, Q., Song, Y., Wei, Z., Lin, H. *et al*. (2022) A super pan-genomic landscape of rice. *Cell Res.* **32**, 878–896.

Sun, P., Zhang, W., Wang, Y., He, Q., Shu, F., Liu, H., Wang, J. *et al*. (2016) *OsGRF4* controls grain shape, panicle length and seed shattering in rice. *J. Integr. Plant Biol.* **58**, 836–847.

Thiemele, D., Boisnard, A., Ndjiondjop, M.N., Cheron, S., Sere, Y., Ake, S., Ghesquiere, A. *et al*. (2010) Identification of a second major resistance gene to Rice yellow mottle virus, RYMV2, in the African cultivated rice species, *O. glaberrima*. *Theor. Appl. Genet.* **121**, 169–179.

Tonnessen, B.W., Manosalva, P., Lang, J.M., Baraoidan, M., Bordeos, A., Mauleon, R., Oard, J. *et al*. (2015) Rice phenylalanine ammonia-lyase gene *OsPAL4* is associated with broad spectrum disease resistance. *Plant Mol. Biol.* **87**, 273–286.

Trapnell, C., Williams, B.A., Pertea, G., Mortazavi, A., Kwan, G., van Baren, M.J., Salzberg, S.L. *et al*. (2010) Transcript assembly and quantification by RNA-Seq reveals unannotated transcripts and isoform switching during cell differentiation. *Nat. Biotechnol.* **28**, 511–515.

van Ittersum, M.K., van Bussel, L.G., Wolf, J., Grassini, P., van Wart, J., Guilpart, N., Claessens, L. *et al*. (2016) Can sub-Saharan Africa feed itself? *Proc. Natl. Acad. Sci. U. S. A.* **113**, 14964–14969.

Win, K.T., Yamagata, Y., Doi, K., Uyama, K., Nagai, Y., Toda, Y., Kani, T. *et al*. (2017) A single base change explains the independent origin of and selection for the nonshattering gene in African rice domestication. *New Phytol.* **213**, 1925–1935.

Wu, W., Liu, X., Wang, M., Meyer, R.S., Luo, X., Ndjiondjop, M.N., Tan, L. *et al*. (2017) A single-nucleotide polymorphism causes smaller grain size and loss of seed shattering during African rice domestication. *Nat. Plants*, **3**, 17064.

Yoon, J., Cho, L.H., Antt, H.W., Koh, H.J. and An, G. (2017) KNOX protein OSH15 induces grain shattering by repressing lignin biosynthesis genes. *Plant Physiol.* **174**, 312–325.

Yoon, J., Cho, L.H., Kim, S.L., Choi, H., Koh, H.J. and An, G. (2014) The BEL1-type homeobox gene *SH5* induces seed shattering by enhancing abscission-zone development and inhibiting lignin biosynthesis. *Plant J.* **79**, 717–728.

Zhang, H., Zhou, J.F., Kan, Y., Shan, J.X., Ye, W.W., Dong, N.Q., Guo, T. *et al*. (2022) A genetic module at one locus in rice protects chloroplasts to enhance thermotolerance. *Science*, **376**, 1293–1300.

Zhang, X., Madi, S., Borsuk, L., Nettleton, D., Elshire, R.J., Buckner, B., Janick-Buckner, D. *et al*. (2007) Laser microdissection of narrow sheath mutant maize uncovers novel gene expression in the shoot apical meristem. *PLoS Genet.* **3**, e101.

Zhou, Y., Lu, D., Li, C., Luo, J., Zhu, B.F., Zhu, J., Shangguan, Y. *et al*. (2012) Genetic control of seed shattering in rice by the APETALA2 transcription factor *shattering abortion1*. *Plant Cell*, **24**, 1034–1048.

Supporting information

Additional supporting information may be found online in the Supporting Information section at the end of the article.

Figure S1 Schematic diagram of the genotype of T65 and GIL292.
Figure S2 Candidate and characterization of *OgSH11*.
Figure S3 Transcription activity assay of full-length or truncated OgSH11 in yeast.
Figure S4 Characterization of *OsSH11* knockout lines.
Figure S5 Comparison of amino acid sequences between GIL292 and T65.
Figure S6 Haplotype analysis of *SH11* in *O. glaberrima* and *O. barthii*.
Figure S7 Comparison of expression level of genes controlling lignin synthesis between GIL292 and Cas9-1.
Figure S8 *SH11* affected seed shattering via binding the promoter of *GH2*.
Figure S9 Use of *SH11* to improve seed shattering in *O. glaberrima*.
Figure S10 Expression analysis among genes related to cellulose synthesis between T65 and *sh4* mutant.
Figure S11 Comparison of amino acid sequences among several *O. rufipogon*, *O. sativa* and GIL292.

Table S1 Accessions used in this study.
Table S2 Primers used in this study.